Suppression of Radiation-Induced Testicular Germ Cell Apoptosis by 2,5-Hexanedione Pretreatment. II. Gene Array Analysis Reveals Adaptive Changes in Cell Cycle and Cell Death Pathways

Sarah N. Campion,* E. Andres Houseman,† Moses A. Sandrof,* Janan B. Hensley,‡ Yunxia Sui,† Kevin W. Gaido,‡ Zhijin Wu,† and Kim Boekelheide*,[1]

*Department of Pathology and Laboratory Medicine and †Department of Community Health, Brown University, Providence, Rhode Island 02912; and ‡The Hamner Institutes for Health Sciences, Research Triangle Park, North Carolina 27709

[1]To whom correspondence should be addressed at Department of Pathology and Laboratory Medicine, Brown University, Box G-E5, Providence, RI 02912. Fax: (401) 863-9008. E-mail: kim_boekelheide@brown.edu.

Sertoli cells are essential for testicular germ cell maintenance and survival. We made the unexpected observation that x-radiation (x-ray)–induced germ cell loss is attenuated by co-exposure with the Sertoli cell toxicant 2,5-hexanedione (HD). The mechanisms underlying this attenuation of germ cell apoptosis with reduced Sertoli cell support are unknown. The current study was performed to examine alterations in testicular gene expression with co-exposure to HD and x-ray. Adult male rats were exposed to HD (0.33 or 1%) in the drinking water for 18 days followed by x-ray (2 or 5 Gy), resulting in nine treatment groups. Testis samples were collected after 3 h and total messenger RNA was analyzed using Affymetrix Rat Genome 230 2.0 arrays. Normalized log2-expression values were analyzed using LIMMA and summarized using linear contrasts designed to summarize the aggregated effect, in excess of x-ray alteration, of HD across all treatment groups. These contrasts were compared with the overall linear trend expression for x-ray, to determine whether HD effects were agonistic or antagonistic with respect to x-ray damage. Overrepresentation analysis to identify biological pathways where HD modification of gene expression was the greatest was performed. HD exerted a significant influence on genes involved in cell cycle and cell death/apoptosis. The results of this study provide insight into the mechanisms underlying attenuated germ cell toxicity following HD and x-ray co-exposure through the analysis of co-exposure effects on gene expression, and suggest that HD pre-exposure reduces Sertoli cell supported germ cell proliferation thereby reducing germ cell vulnerability to x-rays.

Key Words: testis; x-radiation; 2,5-hexanedione; microarray; co-exposure.

Environmental exposure to hazardous chemicals most often occurs as mixed exposures to more than one toxicant (Boekelheide, 2007). There is an emerging need for improved methods for risk assessment and a better understanding of toxicological consequences of mixed exposures. In addition to more traditional toxicological endpoints, microarray analysis is increasingly used as a tool for examining toxicological effects and mechanisms behind mixed exposures (Bartosiewicz *et al.*, 2001; Hook *et al.*, 2008; Rockett and Dix, 1999). These technologies are valuable because complex mixtures may interact in any number of ways, resulting in antagonistic, additive, or synergistic effects (Carpenter *et al.*, 2002; Groten *et al.*, 2001), complicating risk assessment of mixed exposures. When assessing mixture effects in the testis, there is the added complexity of the paracrine-interacting cell types that are necessary for successful spermatogenesis. Testicular toxicants may selectively target a single cell type, such as Sertoli cells or germ cells, with damage to either target resulting in germ cell apoptosis and spermatogenic failure.

Recent research in our laboratory has begun to investigate the consequences of mixed exposures in the testis. 2,5-hexanedione (HD) and x-radiation (x-ray) were used to establish an adult rat model of testicular co-exposure toxicity, which involves a 17-day priming exposure to HD in combination with half-body x-ray exposure on day 17 followed by necropsy 12 h later on day 18. X-radiation disrupts spermatogenesis by directly targeting germ cells. Exposure to x-ray causes free radical–induced DNA breaks in actively dividing spermatogonia, resulting in their apoptosis (Hasegawa *et al.*, 1997). HD is a metabolite of the commonly used solvents *n*-hexane and methyl *n*-butyl ketone (2-hexanone) that causes Sertoli cell dysfunction by interfering with Sertoli cell microtubule assembly kinetics (Boekelheide *et al.*, 2003). HD-induced testicular toxicity is unique in that there is a latency period between initiation of exposure and development of histopathologic alterations, with significantly altered testicular morphology apparent only after 2.5–3 weeks of exposure (reviewed by Boekelheide *et al.*, 2003). The chemistry of HD partially explains the delayed toxicity, which is the result of a progression of subcellular events. HD interacts

with tissue nucleophiles, including protein lysyl ε-amines, resulting in pyrrole formation and accumulation, followed by oxidation and cross-linking (reviewed by Boekelheide *et al.*, 2003). At the end of an 18-day exposure period, as used in our co-exposure paradigm, HD-treated testes exhibit an increase in retained spermatid heads but no increase in germ cell apoptosis at the dose levels used (0.33 and 1%) (Moffit *et al.*, 2007). More severe effects, such as vacuolization, decreased seminiferous tubule fluid formation, and germ cell apoptosis, are observed at later time points (4–5 weeks) after initiating exposure (Boekelheide *et al.*, 2003). Sertoli cells are essential for germ cell maintenance and survival, yet surprisingly, the level of germ cell apoptosis in the testes of rats co-exposed to HD and x-ray was significantly lower than that observed in rats exposed to x-ray alone. This HD-dependent attenuated germ cell death response was stage specific, with a significantly higher degree of apoptosis observed at stages II/III in x-ray alone compared with HD and x-ray combined exposure. These findings are reported in a companion paper by Yamasaki *et al.* (2010)

The goal of the current study was to improve our understanding of this attenuated co-exposure toxicity and identify potential mechanisms by examining global gene expression changes. Because HD pretreatment significantly altered the extent of acute x-ray–induced germ cell apoptosis, this study focused on the degree to which HD attenuated or enhanced the x-ray–induced deviation from the control level for both downregulated and upregulated gene expression. The primary goal of this data analysis approach was to determine if there is a trend toward enhancement or attenuation of x-ray–induced gene alterations by the priming exposure to HD, and to identify those genes that were either enhanced or attenuated. We found that HD significantly affected x-ray–induced expression of genes involved in cell cycle/cell division process, cell cycle/G1/S phase transition, and cell death/apoptosis.

MATERIALS AND METHODS

Animals. Adult male Fischer 344 rats weighing 200–250 g were purchased from Charles River Laboratories (Wilmington, MA). Upon arrival, rats were acclimated for 1 week prior to use and maintained in a temperature- and humidity-controlled environment with a 12-h alternating dark-light cycle. All rats were housed in community cages with free access to water and Purina Rodent Chow 5001 (Farmer's Exchange, Framingham, MA). The Brown University Institutional Animal Care and Use Committee approved all experimental animal protocols in compliance with National Institute of Health guidelines.

Toxicant exposure. Using a previously established treatment protocol (Markelewicz *et al.*, 2004), HD was administered in drinking water *ad libitum* for 18 days at concentrations of 0.33 and 1%. On day 18, animals (*n* = 4 for each treatment group) were exposed to half-body radiation at a single dose of 2 or 5 Gy by a dose rate of 0.31 Gy/min using a RT 250 Philips kVp x-ray machine (Philips, Hamburg, Germany). The dose rate was estimated using a Radcal radiation monitor, model 2026C (Monrovia, CA). At 3 h after treatment with x-ray, following continued HD exposure, rats were euthanized

by CO_2 asphyxiation and half of the right testis was homogenized in Tri Reagent (Sigma-Aldrich, St Louis, MO), snap frozen in liquid nitrogen, and stored at $-80°C$. The remaining testis tissue was fixed in neutral-buffered formalin for histological examination.

RNA isolation and microarray hybridization. RNA was isolated from testes homogenized in Tri Reagent using the RNeasy Mini Kit (Qiagen, Valencia, CA) following manufacturer's protocol. Complementary DNA (cDNA) was synthesized from 2.5 μg total RNA and purified using the Affymetrix One-Cycle Target Labeling and Control Reagents kit (Affymetrix, Santa Clara, CA) according to manufacturer's protocol. Equal amounts of purified cDNA per sample were used as the template for subsequent *in vitro* transcription reactions for complementary RNA (cRNA) amplification and biotin labeling using the Affymetrix GeneChip IVT labeling kit (Affymetrix) included in the One-Cycle Target Labeling kit (Affymetrix). The cRNA was purified and fragmented according to the protocol provided with the GeneChip Sample Cleanup module (Affymetrix). All GeneChip arrays (Rat Genome 230 2.0 arrays) were hybridized, washed, stained, and scanned using the Complete GeneChip Instrument System according to the Affymetrix Technical Manual.

Microarray data analysis. Affymetrix CEL files were preprocessed using the R package GCRMA from Bioconductor to obtain genome-level expression values. The probe-level raw intensities were background corrected by GCRMA, quantile normalized and then summarized into log2-expression measures by Robust Multiarray Analysis. The resulting gene expression values for each of 31,099 genes were merged with netaffx build 29 of Rat Genome 230 2.0 annotation file. Associations with exposure were subsequently analyzed using standard linear model techniques; however, specific contrasts were used to aid interpretation in the context of the co-exposure design. A 3 × 3 factorial study design was used to facilitate the detection of nonlinear effects of exposure and interactions of co-exposure on messenger RNA (mRNA) expression. Because nine model degrees-of-freedom were inherent in the design, multiple patterns of exposure were possible, with some hard to characterize (notably those involving both nonlinearities and interaction). In order to account for non-monotonicity in gene responses and summarize the HD effects above and beyond x-ray, a saturated linear model was used. Univariate (gene-specific) linear models were fit using the R/Bioconductor package *limma* (Smyth, 2004). To summarize linear model results, in particular to simplify the inputs for gene-set pathway analysis, the effects of HD in excess of x-ray were aggregated as the sum of all HD effects over the nine exposure cells. This is equivalent to the sum of the HD effects in the six cells having nonzero HD exposure, and reduces to 3× the sum of the two HD main effects + the four interaction terms (using the standard ANOVA treatment parameterization with the unexposed group as the reference level). The resulting summary statistic has the interpretation of an estimated aggregate HD effect in excess of x-ray, for example, upregulation (positive) or downregulation (negative) by HD. Additionally, the overall linear trend in x-ray was summarized by fitting the equivalent saturated model reparameterized using polynomials in exposure dose (i.e., linear and quadratic terms for each exposure together with their interactions), and extracting the linear x-ray term. To control for multiple comparisons, Q-values representing false discovery rates (FDR) were computed from the collection of all 31,099 *p* values using the *qvalue* package in R (Storey and Tibshirani, 2003).

Pathways analysis. Functional classification of the differentially expressed genes was performed using the Ingenuity Pathways Analysis (IPA) knowledgebase (Ingenuity Systems, Redwood City, CA, IPA 6 content version 1602). The highest and middle-level functional categories of Ingenuity's "Molecular and Cellular Functions" were used to define the gene sets (Supplementary table 1). Pathways analysis was performed using a one-tailed Fisher's exact test (i.e., testing only for overrepresentation and ignoring underrepresentation, the latter of which is not readily interpretable). Genes were considered to be significantly over- or underexpressed with HD exposure (in excess of x-ray), if the HD summary contrast described above had Q-value less than 0.05. Pathways were ranked by *p* value and those with the lowest *p* values were selected for qualitative comparison.

RESULTS

Overview

Rats were euthanized 3 h after x-ray, a time point prior to detection of germ cell apoptosis (Yamasaki *et al.*, 2010), in order to identify early changes in gene expression that precede the histopathologic manifestations of injury. Previous characterization of these histopathologic manifestations of injury at later time points surprisingly revealed that the priming exposure to HD, a Sertoli cell toxicant, attenuated the x-ray–induced germ cell toxicity across all dose combinations (Yamasaki *et al.*, 2010). Because this HD pretreatment significantly modified the extent of acute x-ray–induced germ cell apoptosis, we focused on HD modification of x-ray–induced gene expression alterations in order to get a global view of the HD effects on gene expression. To determine how HD contributes to the gene expression profile during co-exposure, the HD effects were summarized across all treatment groups. From this model, we were able to estimate the degree to which HD modifies the x-ray–induced gene expression alterations. After extracting this contrast of interest, overrepresentation analysis to test for pathway-specific effects of HD on top of x-ray was performed using a one-tailed Fisher's exact test.

Estimates of HD effects on gene expression

The 3 × 3 factorial study design of combined exposure to three different dose levels of HD (0, 0.33, and 1%) with three different dose levels of x-ray (0, 2, and 5 Gy), resulted in a total of nine different treatment groups: 0 HD/0 x-ray (control), 0 HD/2 Gy x-ray, 0 HD/5 Gy x-ray, 0.33 HD/0 x-ray, 0.33 HD/2 Gy x-ray, 0.33 HD/5 Gy x-ray, 1 HD/0 x-ray, 1 HD/2 Gy x-ray, 1 HD/5 Gy x-ray. Upon initial analysis, many genes were found to exhibit nonlinear trends; for example, the expression level for a gene was elevated at the low dose and decreased at the high dose. Consequently, it was necessary to summarize the HD effect in a way that accommodates nonmonotonicity. As described in the "Materials and Methods" section, a summary effect of HD in excess of x-ray was constructed by adding together the four interaction terms and 3× the sum of the two HD main effects (using the standard ANOVA treatment parameterization). The resulting statistic estimates the extent to which HD modifies gene expression above and beyond the x-ray–induced gene expression for each gene during co-exposure. This approach facilitates the identification of genes that exhibit HD modification of x-ray damage. Linear models were fit using LIMMA.

Significant modification of x-ray–induced gene expression alterations by HD pretreatment (FDR < 0.05) were observed for 55 genes (Table 1). X-ray linear effects on gene expression (obtained using polynomial parameterization of a saturated model, as described in the "Materials and Methods" section) are included to provide an indication of the expression induced by x-ray during co-exposure so that we can understand if the HD effect on top of x-ray is an attenuation or enhancement of

these changes. A full list of all genes whose mRNA expression was significantly altered by x-ray can be found in Supplementary table 1. The type of interaction listed in Table 1 indicates how HD and x-ray together influence the expression of the gene. An agonistic interaction indicates that HD and x-ray alter the gene expression in the same way (either both increase or both decrease), which may be either additive or synergistic. An antagonistic interaction indicates opposing HD and x-ray effects, with one toxicant increasing gene expression, whereas the other decreases expression. These two different types of interactions are illustrated in Figure 1. Six of these genes were positively modified by HD. IER3 (immediate early response 3) and ANGPTL4 (angiopoietin-like 4) were the two genes most positively modified by HD. A negative modification of x-ray–induced gene alterations by HD was observed for the 49 other genes, with GHSR (growth hormone secretagogue receptor) and CLCA2 (chloride channel calcium activated 2) being strongly modified by HD in a negative way. Shown in Figure 2 are the gene expression profiles across all nine treatment groups for those four genes significantly modified by HD, as well as some representative genes significantly altered by x-ray during co-exposure (CCNG1, BBC3, and AEN). The example of ANGPTL4 expression in Figure 1 illustrates a negative linear x-ray effect on gene expression, showing a trend of decreasing gene expression as the x-ray dose increases from 0 to 5 Gy. However, a positive HD effect modifies ANGPTL4 gene expression, resulting in an attenuation of the x-ray–induced downregulation. Alternatively, CLCA2 demonstrates an enhancement of x-ray–induced downregulation with HD co-exposure.

Pathways analysis

Overrepresentation analysis was performed to identify biological pathways where HD exhibits the greatest influence on gene expression. The molecular and cellular functions as defined from within the IPA knowledgebase were used to determine the gene sets used for further analysis. A total of 132 gene sets, generated by combining the highest and middle-level functional categories from Ingenuity, were used for pathways analysis (Supplementary table 2). A list of the Ingenuity-annotated pathways in which each of the 55 significantly HD-modified genes (Table 1) is known to participate is provided in Supplementary table 3. Setting the threshold for significance at FDR < 0.05 for the contrast extracted from linear model results, a one-tailed Fisher's exact test was performed to identify pathways that were greatly influenced by HD and related to HD effects on x-ray damage during co-exposure. The one-sided *p* values listed in Table 2 represent nominal *p* values that have not been adjusted for multiple testing. Note, however, that there is substantial overlap in gene sets, which would result in correlation among test results and render many common forms of adjustment as overly conservative. An overall test of altered expression among Ingenuity-defined molecular and cellular function genes ("All Ingenuity Molecular and Cellular

TABLE 1
Genes Significantly Modified by HD Co-exposure

Gene symbol	Gene description	HD effect	Linear x-ray effect	Type of interaction
IER3	Immediate early response 3	6.7233	−0.0574	Antagonistic
ANGPTL4	Angiopoietin-like 4	6.0360	−0.2983	Antagonistic
CTGF	Connective tissue growth factor	3.6301	−0.1609	Antagonistic
ERRFI1	ERBB receptor feedback inhibitor 1	1.9441	−0.0471	Antagonistic
TLE3	Transducin-like enhancer of split 3 (E(sp1) homolog, Drosophila)	1.8419	−0.0077	Antagonistic
MLF2	Myeloid leukemia factor 2	1.0791	0.0135	Agonistic
CD53	CD53 molecule	−0.3673	0.0063	Antagonistic
SSRP1	Structure-specific recognition protein 1	−0.3705	−0.0393	Agonistic
THAP4	THAP domain containing 4	−0.4876	−0.0301	Agonistic
MBD3	Methyl-CpG-binding domain protein 3	−0.5390	−0.0220	Agonistic
PRKAG2	Protein kinase, AMP-activated, gamma 2 noncatalytic subunit	−0.5841	−0.0284	Agonistic
CAMSAP1	Calmodulin-regulated spectrin-associated protein 1	−0.6200	−0.0391	Agonistic
RANBP10	RAN-binding protein 10	−0.7035	0.0026	Antagonistic
NASP	Nuclear autoantigenic sperm protein (histone binding)	−0.7701	−0.0432	Agonistic
LRRC48	Leucine-rich repeat containing 48	−0.7934	−0.0725	Agonistic
GPI	Glucose phosphate isomerase	−0.8050	−0.1152	Agonistic
FBP1	Fructose-1,6-bisphosphatase 1	−0.8497	−0.0416	Agonistic
DHRSX	Dehydrogenase/reductase (SDR family) X-linked	−0.8555	−0.0908	Agonistic
JTV1	JTV1 gene	−0.8961	−0.0647	Agonistic
RGD1306603	—	−0.9134	−0.0432	Agonistic
ITPKA	Inositol 1,4,5-trisphosphate 3-kinase A	−0.9262	−0.0571	Agonistic
RGD1311084	Similar to 1700113K14Rik protein	−0.9977	−0.0894	Agonistic
RGD1309730	Similar to RIKEN cDNA B230118H07	−0.9983	−0.0825	Agonistic
PGAM2	Phosphoglycerate mutase elevated 2	−1.0061	−0.0485	Agonistic
DNMBP	Dynamin-binding protein	−1.0160	−0.0360	Agonistic
PASK	PAS domain containing serine/threonine kinase	−1.0413	−0.0475	Agonistic
MRPS11	Mitochondrial ribosomal protein S11	−1.0454	−0.0264	Agonistic
RCG_20380	Hypothetical protein LOC100125367	−1.0698	−0.0177	Agonistic
DDI2	DDI1, DNA-damage inducible 1, homolog 2 (Saccharomyces cerevisiae)	−1.1447	−0.0276	Agonistic
CNTF	Ciliary neurotrophic factor	−1.1486	−0.0537	Agonistic
FOXK1	Forkhead box K1	−1.1508	−0.0395	Agonistic
H2AFJ	H2A histone family, member J	−1.1984	−0.0711	Agonistic
RNPEP	Arginyl aminopeptidase (aminopeptidase B)	−1.2364	−0.0427	Agonistic
HDDC3	HD domain containing 3	−1.2622	−0.1110	Agonistic
PRSS21	Protease, serine, 21 (testisin)	−1.2652	−0.0599	Agonistic
SHANK3	SH3 and multiple ankyrin repeat domains 3	−1.2974	−0.0321	Agonistic
PITPNM1	Phosphatidylinositol transfer protein, membrane-associated 1	−1.3852	−0.1325	Agonistic
CYGB	Cytoglobin	−1.3958	0.0049	Antagonistic
MAP3K11	Mitogen-activated protein kinase kinase kinase 11	−1.4775	−0.1093	Agonistic
PEX14	Peroxisomal biogenesis factor 14	−1.4910	−0.0197	Agonistic
DNAH1	Dynein, axonemal, heavy chain 1	−1.5618	−0.1265	Agonistic
COMP	Cartilage oligomeric matrix protein	−1.6105	−0.0754	Agonistic
LMOD2	Leiomodin 2 (cardiac)	−1.6165	−0.0933	Agonistic
LOC499124	Mouse zinc finger protein 14-like	−1.6318	−0.0278	Agonistic
CAPG	Capping protein (actin filament), gelsolin-like	−1.6775	−0.1963	Agonistic
COL6A1	Collagen, type VI, alpha 1	−1.7034	−0.0436	Agonistic
HSPB1	Heat shock 27 kDa protein 1	−2.0133	−0.0698	Agonistic
DPP7	Dipeptidyl-peptidase 7	−2.0200	−0.1500	Agonistic
MACROD1	MACRO domain containing 1	−2.0658	−0.1446	Agonistic
ALKBH2	alkB, alkylation repair homolog 2 (Escherichia coli)	−2.1629	−0.0629	Agonistic
CFC1	Cripton, FRL-1, cryptic family 1	−2.5058	−0.0155	Agonistic
LOC683980	Similar to keratinocytes associated protein 3	−2.9492	−0.1152	Agonistic
LOXL1	Lysyl oxidase-like 1	−3.1699	−0.1629	Agonistic
CLCA2 /// CLCA4L	Chloride channel calcium activated 2 /// chloride channel calcium activated 4-like	−3.2185	−0.3286	Agonistic
GHSR	Growth hormone secretagogue receptor	−3.3223	−0.0963	Agonistic

Note. The genes included in this table meet the significance threshold of FDR < 0.05 for the HD Effect. An agonistic interaction indicates an HD effect and x-ray effect in the same direction, whereas an antagonistic interaction indicates an HD effect and x-ray effect in opposing directions.
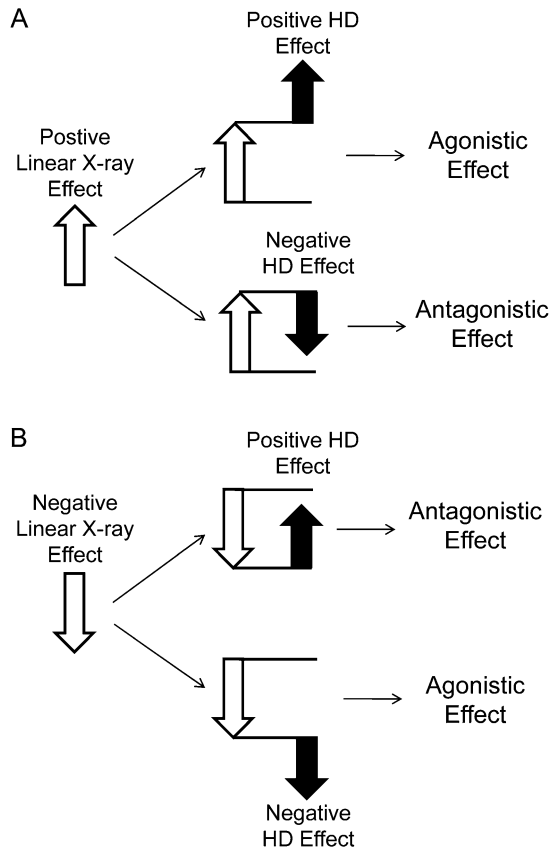
A

B

FIG. 1. HD and x-ray interactions at the gene level. Gene expression alterations were summarized across all nine treatment groups and a linear x-ray effect (open arrows) and an HD effect (black arrows) on co-exposure gene expression were determined. On top of a positive linear x-ray effect (A), a positive HD effect represents an agonistic effect on gene expression, whereas a negative HD effect is an antagonistic effect on gene expression. Similarly, on top of a negative linear x-ray effect (B), a positive HD effect is antagonistic, whereas a negative HD effect is agonistic.

Function Pathways''), considered in isolation of the tests for overrepresentation in specific gene subsets, produces both nominal and adjusted $p = 0.0073$, thus suggesting significant disruption, by HD in excess of x-ray, of important cellular and molecular systems (Supplementary figure 1). Nominal p values for the remaining gene subsets are provided for the purpose of ranking biological pathways for exploratory discovery and hypothesis generation.

The 20 most overrepresented pathways are listed in Table 2. These are predominantly involved in cell cycle, cellular growth and proliferation, DNA replication, recombination and repair, cell death, and lipid and carbohydrate metabolism. Heatmaps of the gene expression values of the top three pathways demonstrate the effect of HD co-exposure across the genes within the pathways (Supplementary figures 2–4). The pathways most affected by HD are cell cycle/cell division process (Supplementary fig. 2), cell cycle/G1/S phase transition (Supplementary fig. 3), and cell death/apoptosis (Supplementary fig. 4). Within the cell cycle/cell division process pathway,

the most strongly upregulated genes include IER3, EGR1 (early growth response 1), and STAT3 (signal transducer and activator of transcription 3), whereas PITX2 (paired-like homeodomain 2), XRCC4 (x-ray repair complementing defective repair in Chinese hamster cells 4), and MAP3K11 (mitogen-activated protein kinase kinase kinase 11) are among those strongly downregulated. Similar genes fall in the cell cycle/G1/S phase transition pathway, with prominently affected genes including NFKBIA (nuclear factor of kappa light polypeptide gene enhancer in B cells inhibitor, alpha), JUN (jun oncogene), CDKN1A (cyclin-dependent kinase inhibitor 1A), and several cyclins (CCNA1, CCND1, and CCNE1). ANGPTL4, EGR1, CTGF (connective tissue growth factor), BBC3 (Bcl2-binding component 3), and HSPB1 (heat shock 27 kDa protein 1) are among the many affected genes involved in cell death/apoptosis.

DISCUSSION

In the present study, microarray analysis was used to identify changes in gene expression underlying the pathological changes that occur when adult rats are co-exposed to HD and x-ray. In our previous study, it was found that an 18-day priming exposure to the Sertoli cell toxicant HD resulted in a surprising attenuation of x-ray–induced germ cell apoptosis. Sensitization with HD exposure appears to induce an adaptive response, which alters the sensitivity of germ cells to x-rays. Using integrated bioinformatic techniques to analyze dose-response and co-exposure effects on gene expression, we identified individual genes and biological pathways underlying this attenuated germ cell response.

When studying mixed exposures, it is common practice to compare the gene expression profile after co-exposure to the gene expression profiles after exposure to the individual components of the mixture. With our study design involving multiple dose levels of each toxicant, this type of comparison could not be easily performed because of the complexity introduced by the dose-dependent effects of co-exposure. The phenotypic response of attenuated apoptosis following co-exposure was most unique; therefore, we focused primarily on the gene expression profile of the co-exposure group, dissecting the contribution of each toxicant to the co-exposure response.

HD pretreatment attenuated the downregulation by x-rays of IER3, ANGPTL4, CTGF, and ERRFI1 among other genes. IER3 is an immediate early response gene that has been shown to have an anti-apoptotic function in some cell types, promoting cell survival (Wu, 2003). ANGPTL4 is an apoptosis survival factor for endothelial cells and also plays a role in lipid metabolism and insulin sensitivity (Kim *et al.*, 2000; Xu *et al.*, 2005). When secreted, CTGF stimulates proliferation of various cell types and extracellular matrix component production. CTGF can also be expressed as an intracellular protein
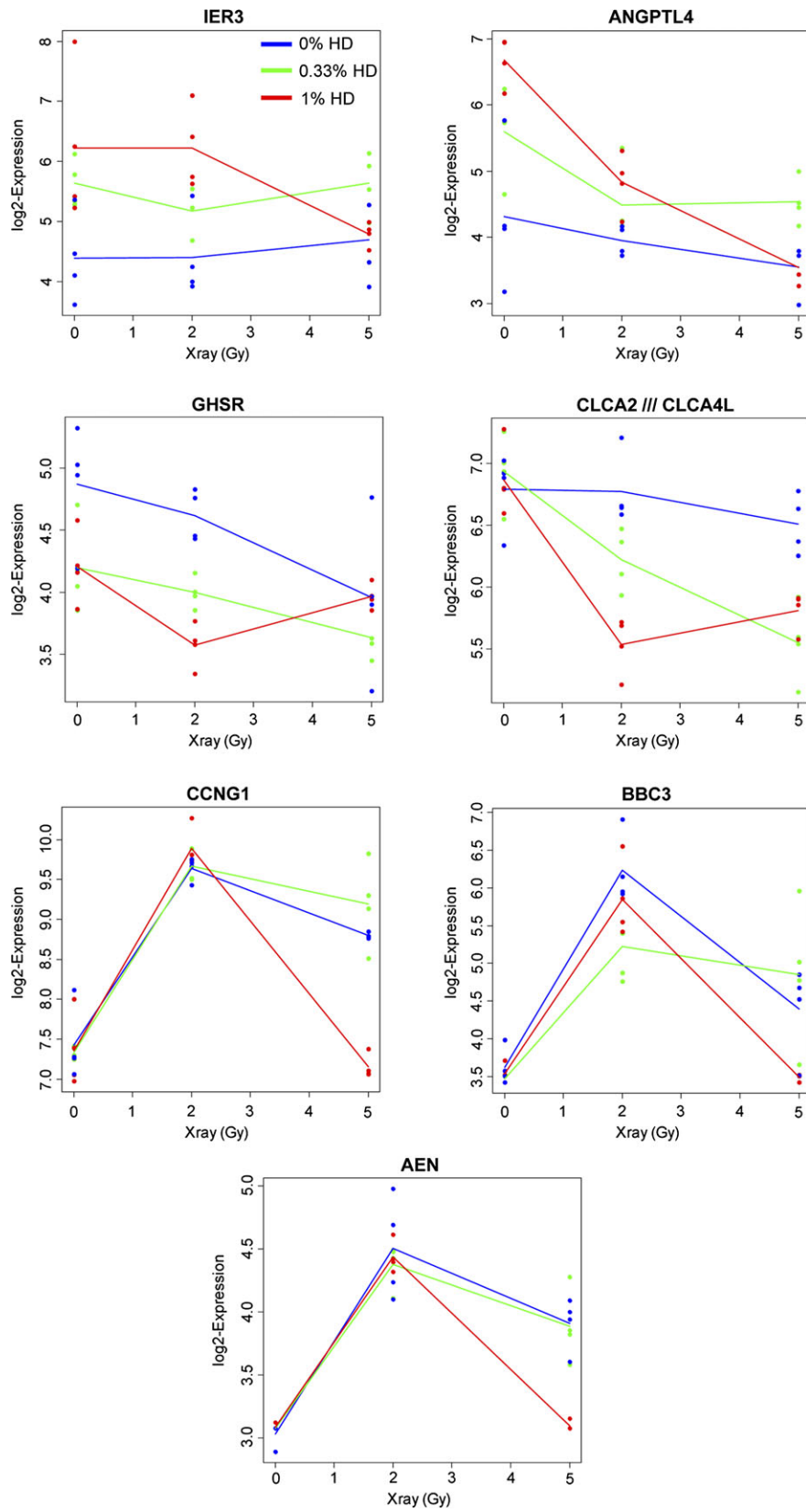
FIG. 2. Co-exposure effects on gene expression. Relative gene expression following exposure to 0% (blue line), 0.33% (green line) or 1% HD (red line) in combination with 0, 2 or 5 Gy x-ray was determined by microarray analysis.

TABLE 2
Biological Pathways Influenced by HD

Pathway number	Pathway name	Odds ratio	p Value
—	All Ingenuity molecular and cellular function pathways	2.0103	0.0073
18	Cell cycle/cell division process	2.7952	0.0130
22	Cell cycle/G1/S phase transition	6.8666	0.0378
26	Cell death/apoptosis	1.9380	0.0527
6	Carbohydrate metabolism/metabolic process	3.6211	0.0563
17	Cell cycle/cell cycle progression	2.5197	0.0591
81	DNA replication, recombination, and repair/metabolism	3.3731	0.0664
79	DNA replication, recombination, and repair/fragmentation	4.7104	0.0725
19	Cell cycle/cell stage	2.3598	0.0731
96	Lipid metabolism/metabolism	3.0340	0.0845
78	DNA replication, recombination, and repair/degradation	4.0847	0.0920
62	Cellular development/hypertrophy	4.0534	0.0932
71	Cellular growth and proliferation/hypertrophy	4.0534	0.0932
95	Lipid metabolism/metabolic process	2.8567	0.0966
42	Cell signaling/protein kinase cascade	2.6618	0.1126
72	Cellular growth and proliferation/proliferation	1.6778	0.1163
27	Cell death/cell death	1.6345	0.1166
7	Carbohydrate metabolism/quantity	3.3715	0.1256
61	Cellular development/growth	3.3498	0.1269
97	Lipid metabolism/modification	3.3283	0.1282
58	Cellular development/developmental disorder	3.2862	0.1308

in a cell cycle–dependent manner, causing cell cycle arrest (Kubota *et al.*, 2000). CTGF can interact with integrins on the Sertoli cell surface and may regulate essential Sertoli cell-germ cell interactions (O'Donnell *et al.*, 2009). ERRFI1 (ERBB receptor feedback inhibitor 1) is an immediate early response gene induced during periods of cell stress and can function as a tumor suppressor (Zhang and Vande Woude, 2007). HD pretreatment also exerted a significant negative effect on many genes. In this group of genes, nearly all negative modifications by HD were an enhancement of x-ray–induced downregulation. Several of these genes (e.g., NASP, HSPB1, and ALKBH2) are involved in DNA replication, recombination and repair as well as cell death/apoptosis (e.g., GPI, CNTF, MAP3K11, COMP, and HSPB1). These changes are not surprising because x-ray exposure results in DNA damage that ultimately results in germ cell apoptosis. HD pretreatment also enhances the x-ray–induced downregulation of several genes whose products are involved in cellular growth and proliferation/cell cycle (e.g., SSRP1, NASP, GPI, PITPNM1, MAP3K11, and LOXL1) and also carbohydrate and lipid metabolism (PITPNM1, GHSR, CYGB, GPI, FBP1, ITPKA, and CNTF). Changes in carbohydrate and lipid metabolism have implications for reduced Sertoli cell support of and communication with germ cells.

Some other genes that are strongly further downregulated by HD co-exposure are LOXL1, GHSR, and PRSS21 (protease,

serine, 21). GHSR and LOXL1 exhibit some of the greatest negative HD effects and recent studies have begun to reveal a role for the products of these genes in the male reproductive system. LOXL1−/− male mice exhibit decreased fertility and decreased sperm production, although the mechanisms behind these effects are unknown (Wood *et al.*, 2009). Ghrelin is the endogenous ligand for GHSR. Locally expressed ghrelin in the testis inhibits hCG- and cAMP-stimulated testosterone secretion *in vitro* and also causes a reduction in steroidogenic gene expression (Lorenzi *et al.*, 2009). PRSS21, also called TEST1 or TESTISIN, is a serine protease expressed by premeiotic primary spermatocytes in the cytoplasm and on the plasma membrane and is suggested to be involved in germ cell maturation (Hooper *et al.*, 1999). Whereas the exact role of TEST1 is not known, it may participate in proteolytic events necessary for germ cell migration, or in the exchange of soluble factors or cell surface interactions between germ cells and Sertoli cells (Hooper *et al.*, 1999).

In addition to focusing on individual genes altered by HD on top of x-ray, pathways analysis was used to gain a better understanding of the molecular changes underlying the co-exposure response. Biological pathways with the greatest modification of gene expression by HD exposure were identified, and within these pathways several genes of interest were revealed. A significant influence of HD on genes involved in cell cycle was discovered. Looking at the genes within these pathways below the threshold of $p < 0.05$, most are negatively affected by HD, suggesting that there may be cell cycle arrest. HD-mediated attenuation of genes that promote cell proliferation may cause a reduction in germ cell proliferation, rendering them more resistant to x-ray exposure. HD-exposed rats exhibited increased duration of the spermatogenic cycle that was attributed to reduced progression of 5-bromodeoxyuridine (BrdU)-labeled cells (Rosiepen *et al.*, 1995). Compromised Sertoli cell-mediated transport of germ cells may be the cause for decreased BrdU labeling during specific stages. However, impaired division of spermatogonia may also explain the reduction in BrdU-labeled germ cells. Among the other genes within these cell cycle–related gene sets, there is an HD-mediated enhancement of CDKN1A (cyclin-dependent kinase inhibitor 1A, p21), a cell cycle inhibitor that is controlled by p53. p53-dependent cell cycle arrest in response to cell stress is mediated by CDKN1A/p21, and this growth arrest mediated by p21 can inhibit apoptosis (Yu and Zhang, 2005). Alternatively, there is decreased expression of several cyclins (CCNA1, CCNB1, CCNE1, CCNG1, and CCND2) and other genes involved in the promotion of cell cycle progression following co-exposure. For example, NASP (nuclear autoantigenic sperm protein [histone binding]), which is decreased by HD, is regulated by the cell cycle and functions in the transport of histones to the nucleus of dividing cells (Richardson *et al.*, 2000).

The attenuation of germ cell apoptosis was the most remarkable histopathologic observation following co-exposure to HD and x-ray, therefore it was not surprising that the cell

death/apoptosis pathway was overrepresented among significant genes. Examining the genes within this pathway, as well as considering those genes significantly altered by x-ray exposure (Supplementary table 1), there is a strong trend toward attenuation of x-ray–induced proapoptotic genes by HD co-exposure. CCNG1 (cyclin G1), BBC3 (Bcl2-binding component 3), and AEN (apoptosis-enhancing nuclease) are all proapoptotic genes that were significantly increased by x-ray exposure with HD-mediated attenuation following co-exposure. HD co-exposure prevents the induction of CCNG1 caused by x-ray. CCNG1 is a transcriptional target of p53 that regulates p53 and its functions, including apoptosis (Kimura and Nojima, 2002). Under certain cellular conditions, CCNG1 can also negatively regulate p53 and promote cell growth rather than cell cycle arrest (Chen, 2002). As discussed earlier, a decrease in germ cell proliferation, which could be related to attenuated CCNG1 upregulation, may protect germ cells from x-ray. Attenuation of x-ray–induced BBC3 and AEN was also detected by gene array analysis. BBC3, also known as PUMA (p53-upregulated modulator of apoptosis), mediates p53-induced apoptosis by either preventing the action of the antiapoptotic proteins Bcl-2 and Bcl-X_L, or by promoting p53 dissociation from Bcl-X_L, allowing p53 to activate Bax (Wang et al., 2007). AEN enhances apoptosis following ionizing radiation through its DNase activity (Lee et al., 2005). BBC3/PUMA and AEN are increased by 1.7- and 3.2-fold, respectively, after exposure to 5 Gy x-ray, with their expression attenuated to control levels following co-exposure. These notable differences in induction between x-ray alone and co-exposure, along with the documented roles of BBC3/PUMA and AEN in the apoptotic pathways that are activated following radiation exposure, make these genes strong candidates for further investigation. In addition to these modifications of proapoptotic genes, there was HD-dependent enhancement of antiapoptotic genes. NFKBIA (nuclear factor of kappa light polypeptide gene enhancer in B cells inhibitor, alpha), better known as IκBα, functions to inhibit nuclear factor κB (NF-κB) proteins by sequestering them in the cytoplasm in an inactive state (Jacobs and Harrison, 1998) and is enhanced by co-exposure to HD. This enhancement would be expected to reduce apoptosis as NF-κB activation is proapoptotic in the irradiated testis (Rasoulpour and Boekelheide, 2007).

In conclusion, we have derived new insights into the mechanisms underlying the phenotypic effects of HD and x-ray co-exposure by investigating global gene expression in the testis, focusing on the influence of HD on x-ray–induced gene alterations. The less supportive environment induced by HD pretreatment results in adaptation of the germ cells and an increased resistance to subsequent insults by x-ray exposure. The modulation of gene expression caused by HD sensitization corresponds well with the phenotypic characteristics resulting from HD pretreatment. Particularly, the HD-dependent attenuation of several proapoptotic genes correlates with the attenuated germ cell apoptosis. Additional studies are un-

derway to investigate these alterations in apoptotic genes, specifically BBC3/PUMA and AEN. In the current study, gene expression analysis was performed using RNA isolated from whole testis; however, the attenuated apoptosis is stage specific (Yamasaki et al., 2010). More focused studies investigating the expression of these apoptotic genes in specific stages by qRT-PCR, which is more sensitive than microarray analysis, will provide further insight into the current findings. In addition to these alterations in apoptotic genes, HD modulated several signaling pathways of interest, including cell cycle/cell division process and cell cycle/G1/S phase transition that may mechanistically explain this reduced apoptotic response. Abnormal Sertoli cell support of germ cells and altered communication between Sertoli cells and germ cells by HD pretreatment likely contribute to the attenuation of germ cell apoptosis. This may be due to a role of Sertoli cells in regulating germ cell apoptosis following DNA damage. Alternatively, reduced Sertoli cell support may result in decreased germ cell division and therefore, reduced vulnerability to x-rays that target actively dividing cells. Future studies will explore further this possible disruption of germ cell division by HD exposure.

SUPPLEMENTARY DATA

Supplementary data are available online at http://toxsci.oxfordjournals.org/.

FUNDING

REFERENCES

Bartosiewicz, M., Penn, S., and Buckpitt, A. (2001). Applications of gene arrays in environmental toxicology: fingerprints of gene regulation associated with cadmium chloride, benzo(a)pyrene, and trichloroethylene. *Environ. Health Perspect.* **109**, 71–74.

Boekelheide, K. (2007). Mixed messages. *Toxicol. Sci.* **99**, 1–2.

Boekelheide, K., Fleming, S. L., Allio, T., Embree-Ku, M. E., Hall, S. J., Johnson, K. J., Kwon, E. J., Patel, S. R., Rasoulpour, R. J., Schoenfeld, H. A., et al. (2003). 2,5-hexanedione-induced testicular injury. *Annu. Rev. Pharmacol. Toxicol.* **43**, 125–147.

Carpenter, D. O., Arcaro, K., and Spink, D. C. (2002). Understanding the human health effects of chemical mixtures. *Environ. Health Perspect* **110**(Suppl. 1), 25–42.

Chen, X. (2002). Cyclin G: a regulator of the p53-Mdm2 network. *Dev. Cell.* **2**, 518–519.

Groten, J. P., Feron, V. J., and Suhnel, J. (2001). Toxicology of simple and complex mixtures. *Trends Pharmacol. Sci.* **22**, 316–322.

Hasegawa, M., Wilson, G., Russell, L. D., and Meistrich, M. L. (1997). Radiation-induced cell death in the mouse testis: relationship to apoptosis. *Radiat. Res.* **147**, 457–467.

Hook, S. E., Skillman, A. D., Gopalan, B., Small, J. A., and Schultz, I. R. (2008). Gene expression profiles in rainbow trout, Onchorynchus mykiss, exposed to a simple chemical mixture. *Toxicol. Sci.* **102,** 42–60.

Hooper, J. D., Nicol, D. L., Dickinson, J. L., Eyre, H. J., Scarman, A. L., Normyle, J. F., Stuttgen, M. A., Douglas, M. L., Loveland, K. A., Sutherland, G. R., *et al.* (1999). Testisin, a new human serine proteinase expressed by premeiotic testicular germ cells and lost in testicular germ cell tumors. *Cancer Res.* **59,** 3199–3205.

Jacobs, M. D., and Harrison, S. C. (1998). Structure of an IkappaBalpha/NF-kappaB complex. *Cell* **95,** 749–758.

Kim, I., Kim, H. G., Kim, H., Kim, H. H., Park, S. K., Uhm, C. S., Lee, Z. H., and Koh, G. Y. (2000). Hepatic expression, synthesis and secretion of a novel fibrinogen/angiopoietin-related protein that prevents endothelial-cell apoptosis. *Biochem J.* **346**(Pt 3), 603–610.

Kimura, S. H., and Nojima, H. (2002). Cyclin G1 associates with MDM2 and regulates accumulation and degradation of p53 protein. *Genes Cells* **7,** 869–880.

Kubota, S., Hattori, T., Shimo, T., Nakanishi, T., and Takigawa, M. (2000). Novel intracellular effects of human connective tissue growth factor expressed in Cos-7 cells. *FEBS Lett.* **474,** 58–62.

Lee, J. H., Koh, Y. A., Cho, C. K., Lee, S. J., Lee, Y. S., and Bae, S. (2005). Identification of a novel ionizing radiation-induced nuclease, AEN, and its functional characterization in apoptosis. *Biochem. Biophys. Res. Commun.* **337,** 39–47.

Lorenzi, T., Meli, R., Marzioni, D., Morroni, M., Baragli, A., Castellucci, M., Gualillo, O., and Muccioli, G. (2009). Ghrelin: a metabolic signal affecting the reproductive system. *Cytokine Growth Factor Rev* **20,** 137–152.

Markelewicz, R. J., Jr., Hall, S. J., and Boekelheide, K. (2004). 2,5-hexanedione and carbendazim co-exposure synergistically disrupts rat spermatogenesis despite opposing molecular effects on microtubules. *Toxicol. Sci.* **80,** 92–100.

Moffit, J. S., Bryant, B. H., Hall, S. J., and Boekelheide, K. (2007). Dose-dependent effects of sertoli cell toxicants 2,5-hexanedione, carbendazim, and mono-(2-ethylhexyl) phthalate in adult rat testis. *Toxicol. Pathol.* **35,** 719–727.

O'Donnell, L., Pratis, K., Wagenfeld, A., Gottwald, U., Muller, J., Leder, G., McLachlan, R. I., and Stanton, P. G. (2009). Transcriptional profiling of the hormone-responsive stages of spermatogenesis reveals cell-, stage-, and hormone-specific events. *Endocrinology* **150,** 5074–5084.

Rasoulpour, R. J., and Boekelheide, K. (2007). NF-kappaB activation elicited by ionizing radiation is proapoptotic in testis. *Biol. Reprod.* **76,** 279–285.

Richardson, R. T., Batova, I. N., Widgren, E. E., Zheng, L. X., Whitfield, M., Marzluff, W. F., and O'Rand, M. G. (2000). Characterization of the histone H1-binding protein, NASP, as a cell cycle-regulated somatic protein. *J. Biol. Chem.* **275,** 30378–30386.

Rockett, J. C., and Dix, D. J. (1999). Application of DNA arrays to toxicology. *Environ Health Perspect* **107,** 681–685.

Rosiepen, G., Chapin, R. E., and Weinbauer, G. F. (1995). The duration of the cycle of the seminiferous epithelium is altered by administration of 2,5-hexanedione in the adult Sprague-Dawley rat. *J. Androl.* **16,** 127–135.

Smyth, G. K. (2004). Linear models and empirical bayes methods for assessing differential expression in microarray experiments. *Stat. Appl. Genet. Mol. Biol.* **3,** Article3.

Storey, J. D., and Tibshirani, R. (2003). Statistical significance for genomewide studies. *Proc. Natl. Acad. Sci. U.S.A.* **100,** 9440–9445.

Wang, P., Yu, J., and Zhang, L. (2007). The nuclear function of p53 is required for PUMA-mediated apoptosis induced by DNA damage. *Proc. Natl. Acad. Sci. U.S.A.* **104,** 4054–4059.

Wood, H. M., Lee, U. J., Vurbic, D., Sabanegh, E., Ross, J. H., Li, T., and Damaser, M. S. (2009). Sexual development and fertility of Loxl1-/- male mice. *J. Androl.* **30,** 452–459.

Wu, M. X. (2003). Roles of the stress-induced gene IEX-1 in regulation of cell death and oncogenesis. *Apoptosis* **8,** 11–18.

Xu, A., Lam, M. C., Chan, K. W., Wang, Y., Zhang, J., Hoo, R. L., Xu, J. Y., Chen, B., Chow, W. S., Tso, A. W., *et al.* (2005). Angiopoietin-like protein 4 decreases blood glucose and improves glucose tolerance but induces hyperlipidemia and hepatic steatosis in mice. *Proc. Natl. Acad. Sci. U.S.A.* **102,** 6086–6091.

Yamasaki, H., Sandrof, M. A., and Boekelheide, K. (2010). Suppression of radiation-induced testicular germ cell apoptosis by 2,5-hexanedione pre-treatment. I. Histopathological analysis reveals stage-dependence of attenuated apoptosis. *Toxicol. Sci.* Advance Access published on July 8, 2010; doi: 10.1093/toxsci/kfq203.

Yu, J., and Zhang, L. (2005). The transcriptional targets of p53 in apoptosis control. *Biochem. Biophys. Res. Commun.* **331,** 851–858.

Zhang, Y. W., and Vande Woude, G. F. (2007). Mig-6, signal transduction, stress response and cancer. *Cell Cycle* **6,** 507–513.